FINITE ELEMENT ANALYSIS FOR MINIMAL SHAPE

Vinicius Arcaro, Katalin Klinka, Dario Gasparini

This text describes a novel mathematical model that unifies all geometrical minimal shape problems by defining geometrical finite elements. Three types of elements are defined: line, triangle and tetrahedron. By associating a volume for each element type, the elements can be used together in the discretization of a geometrical shape. For each element type, its corresponding isovolumetric element is also defined. The geometrical minimal shape problem is formulated as an equality constrained minimization problem. The importance of this approach is that apparently distinct problems can be treated by a unified framework. The augmented Lagrangian method is used to solve the associated unconstrained minimization problem. A quasi-Newton method is used, which avoids the evaluation of the Hessian matrix. The source and executable computer codes of the algorithm are available for download from the website of one of the authors.

Keywords: element, line, membrane, minimization, nonlinear, optimization, tetrahedron, triangle.

1 Introduction

This text describes a mathematical model that unifies all geometrical minimal shape problems by defining geometrical finite elements. Three types of elements are defined: line, triangle and tetrahedron. The elements can be used together through the unifying concept of volume. For each element type, its corresponding isovolumetric element is also defined. The shape is discretized into line, triangle and tetrahedron elements. The elements are interconnected at their nodal points. The geometrical minimal shape problem is formulated as an equality constrained minimization problem. The augmented Lagrangian method is used to solve the associated unconstrained minimization problem. A quasi-Newton method is used, which avoids the evaluation of the Hessian matrix.

The following conventions apply unless otherwise specified or made clear by the context. A Greek letter expresses a scalar. A lower-case letter represents a column vector.

2 Line element definition

Figure 1 shows the geometry of the line element for a 3D space. The nodes are labeled 1 and 2. The nodal displacements transform the element from its initial state to its final state.

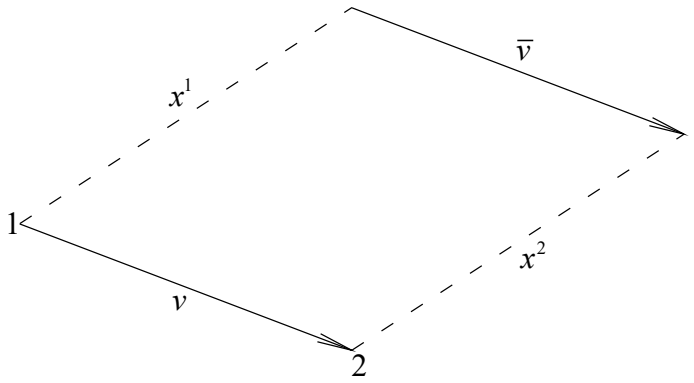

Figure 1

$\bar{v} = v + x^2 - x^1$

2.1 Element initial and final volumes

Let the constant cross-sectional area be α_0. The initial volume can be written as:

$$\phi_e^0 = \alpha_0 \|v\|$$

The final volume can be written as:

$$\phi_e(x) = \alpha_0 \|\bar{v}\|$$

2.2 Gradient of the element final volume

The gradient with respect to the nodal displacements can be written as:

$$\nabla \phi_e(x) = \frac{\alpha_0}{\|\bar{v}\|} \begin{bmatrix} -\bar{v} \\ +\bar{v} \end{bmatrix}$$

3 Triangle element definition

Figure 2 shows the geometry of the triangle element for a 3D space. The nodes are labeled 1, 2 and 3 while traversing the sides in counterclockwise fashion. Each side is labeled with the number of its opposite node. The nodal displacements transform the element from its initial state to its final state.

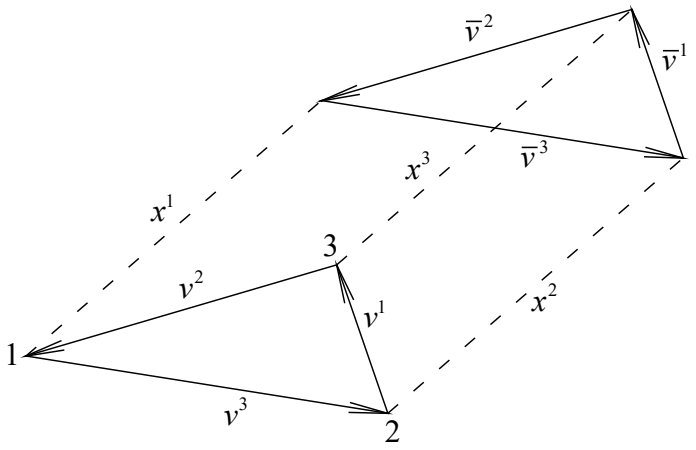

Figure 2

$$\overline{v}^1 = v^1 + x^3 - x^2$$

$$\overline{v}^2 = v^2 + x^1 - x^3$$

$$\overline{v}^3 = v^3 + x^2 - x^1$$

$$w = v^1 \times v^2$$

$$\overline{w} = \overline{v}^1 \times \overline{v}^2$$

The vectors w and $\overline{w}$ are orthogonal to the element in the initial state and final state, respectively. Note that these vectors point toward the observer.

3.1 Element initial and final volumes

Let the constant thickness be λ_0. The initial volume can be written as:

$$\phi_e^0 = \frac{\lambda_0}{2}\|w\|$$

The final volume can be written as:

$$\phi_e(x) = \frac{\lambda_0}{2}\|\overline{w}\|$$

3.2 Gradient of the element final volume

The derivatives of the final volume with respect to the nodal displacements can be written as:

$$\frac{\partial \phi_e(x)}{\partial x_i^j} = \frac{\lambda_0}{2\|\overline{w}\|}\left(\overline{w}_1 \frac{\partial \overline{w}_1}{\partial x_i^j} + \overline{w}_2 \frac{\partial \overline{w}_2}{\partial x_i^j} + \overline{w}_3 \frac{\partial \overline{w}_3}{\partial x_i^j}\right)$$

The vector $\overline{w}$ can be written as function of the nodal displacements as:

$$\overline{w} = w +$$
$$+v^1 \times x^1 + v^2 \times x^2 + v^3 \times x^3 +$$
$$+x^1 \times x^2 + x^2 \times x^3 + x^3 \times x^1$$

$$\begin{bmatrix} \frac{\partial \overline{w}_1}{\partial x_1^j} & \frac{\partial \overline{w}_1}{\partial x_2^j} & \frac{\partial \overline{w}_1}{\partial x_3^j} \\ \frac{\partial \overline{w}_2}{\partial x_1^j} & \frac{\partial \overline{w}_2}{\partial x_2^j} & \frac{\partial \overline{w}_2}{\partial x_3^j} \\ \frac{\partial \overline{w}_3}{\partial x_1^j} & \frac{\partial \overline{w}_3}{\partial x_2^j} & \frac{\partial \overline{w}_3}{\partial x_3^j} \end{bmatrix} = \begin{bmatrix} 0 & -\overline{v}_3^j & \overline{v}_2^j \\ \overline{v}_3^j & 0 & -\overline{v}_1^j \\ -\overline{v}_2^j & \overline{v}_1^j & 0 \end{bmatrix}$$

$$\frac{\partial \phi_e(x)}{\partial x^j} = \frac{\lambda_0}{2\|\overline{w}\|} \begin{bmatrix} +\overline{w}_2 \overline{v}_3^j - \overline{w}_3 \overline{v}_2^j \\ +\overline{w}_3 \overline{v}_1^j - \overline{w}_1 \overline{v}_3^j \\ \overline{w}_1 \overline{v}_2^j - \overline{w}_2 \overline{v}_1^j \end{bmatrix} = \frac{\lambda_0}{2\|\overline{w}\|} \overline{w} \times \overline{v}^j$$

The gradient with respect to the nodal displacements can be written as:

$$\nabla \phi_e(x) = \frac{\lambda_0}{2\|\overline{w}\|} \begin{bmatrix} \overline{w} \times \overline{v}^1 \\ \overline{w} \times \overline{v}^2 \\ -\overline{w} \times \overline{v}^1 - \overline{w} \times \overline{v}^2 \end{bmatrix}$$

4 Tetrahedron element definition

Figure 3 shows the geometry of the tetrahedron element. The base nodes are labeled 1, 2 and 3 while traversing the sides in clockwise fashion looking from the apex, which is labeled 4. The nodal displacements transform the element from its initial state to its final state.

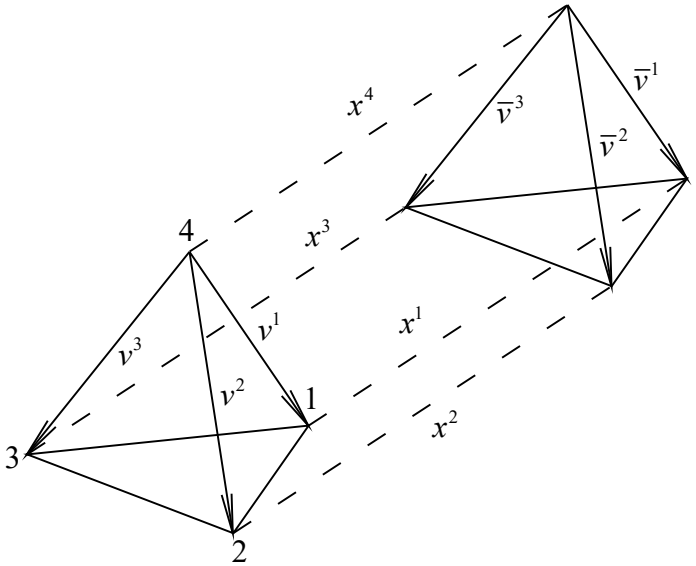

Figure 3

$$\overline{v}^1 = v^1 + x^1 - x^4$$

$$\overline{v}^2 = v^2 + x^2 - x^4$$

$$\overline{v}^3 = v^3 + x^3 - x^4$$

4.1 Element initial and final volumes

The initial volume can be written as:

$$\phi_e^0 = \frac{1}{6}\left(v^1\right)^T \left(v^2 \times v^3\right)$$

The final volume can be written as:

$$\phi_e\left(x\right) = \frac{1}{6}\left(\overline{v}^1\right)^T \left(\overline{v}^2 \times \overline{v}^3\right)$$

Let

$$\delta = \left(v^1\right)^T \left(\overline{v}^2 \times z^3\right) + \left(v^2\right)^T \left(\overline{v}^3 \times z^1\right) + \left(v^3\right)^T \left(\overline{v}^1 \times z^2\right) + \left(z^1\right)^T \left(z^2 \times z^3\right)$$

The final volume expression can be written as:

$$\phi_e\left(x\right) = \phi_e^0 + \frac{\delta}{6}$$

4.2 Gradient of the element final volume

The gradient with respect to the nodal displacements can be written as:

$$\nabla\phi_e\left(x\right) = \frac{1}{6}\begin{bmatrix} \overline{v}^2 \times \overline{v}^3 \\ \overline{v}^3 \times \overline{v}^1 \\ \overline{v}^1 \times \overline{v}^2 \\ -\overline{v}^2 \times \overline{v}^3 - \overline{v}^3 \times \overline{v}^1 - \overline{v}^1 \times \overline{v}^2 \end{bmatrix}$$

5 Constraint function for the isovolumetric element

An element that does not change its volume is desirable for many problem types. Ideally, the volume change should be zero for the isovolumetric element in its final state. Considering ϕ_e^0 as the initial volume, a constraint function associated with the isovolumetric element can be defined by the relative difference between the final and initial volumes.

$$\varphi_e\left(x\right) = \frac{\phi_e\left(x\right) - \phi_e^0}{\phi_e^0}$$

5.1 Severe cancellation

Inaccuracy often results from severe cancellation that occurs when nearly equal values are subtracted [01]. Note that inaccuracy can result from the difference between the final and initial volumes because they can be arbitrarily close for the isovolumetric element. However, severe cancellation can usually be eliminated by algebraic reformulation. The relative difference between the final and initial volumes, reformulated to avoid severe cancellation, can be written for the line, triangle and tetrahedron elements.

5.1.1 Line element

$$z = x^2 - x^1$$

$$\delta = \frac{z^T \left(2v + z\right)}{\left\|v\right\|^2}$$

$$\varphi_e\left(x\right) = \frac{\delta}{\sqrt{1+\delta}+1}$$

5.1.2 Triangle element

$$z = \left(v^1 - x^2\right) \times x^1 + \left(v^2 - x^3\right) \times x^2 + x^3 \times \left(v^1 + v^2 + x^1\right) \Rightarrow \overline{w} = w + z$$

$$\delta = \frac{z^T \left(2w + z\right)}{\left\|w\right\|^2}$$

$$\varphi_e\left(x\right) = \frac{\delta}{\sqrt{1+\delta}+1}$$

5.1.3 Tetrahedron element

$$\delta = \left(v^1\right)^T \left(\overline{v}^2 \times z^3\right) + \left(v^2\right)^T \left(\overline{v}^3 \times z^1\right) + \left(v^3\right)^T \left(\overline{v}^1 \times z^2\right) + \left(z^1\right)^T \left(z^2 \times z^3\right)$$

$$\varphi_e\left(x\right) = \frac{\delta}{\left(v^1\right)^T \left(v^2 \times v^3\right)}$$

5.2 Gradient of the constraint function

The gradient of the constraint function with respect to the nodal displacements of the element can be written as:

$$\nabla \varphi_e\left(x\right) = \frac{1}{\phi_e^0} \nabla \phi_e\left(x\right)$$

5.2.1 Line element

$$\nabla\varphi_e(x)=\frac{1}{\|v\|\|\overline{v}\|}\begin{bmatrix}-\overline{v}\\+\overline{v}\end{bmatrix}$$

5.2.2 Triangle element

$$\nabla\varphi_e(x)=\frac{1}{\|w\|\|\overline{w}\|}\begin{bmatrix}\overline{w}\times\overline{v}^1\\\overline{w}\times\overline{v}^2\\-\overline{w}\times\overline{v}^1-\overline{w}\times\overline{v}^2\end{bmatrix}$$

5.2.3 Tetrahedron element

$$\nabla\varphi_e(x)=\frac{1}{\left(v^1\right)^T\left(v^2\times v^3\right)}\begin{bmatrix}\overline{v}^2\times\overline{v}^3\\\overline{v}^3\times\overline{v}^1\\\overline{v}^1\times\overline{v}^2\\-\overline{v}^2\times\overline{v}^3-\overline{v}^3\times\overline{v}^1-\overline{v}^1\times\overline{v}^2\end{bmatrix}$$

6 The minimal shape problem

The minimal shape problem can be written as an equality constrained minimization problem, with one constraint for each isovolumetric element, as:

$$\text{Min}\sum_e\phi_e(x)$$

Subject to $\varphi_e(x)=0$

6.1 Augmented Lagrangian method

Historically, the quadratic penalty method was the first method used for constrained nonlinear programming. Due to its simplicity, it is still used in practice, although it has an important computational disadvantage. The augmented Lagrangian method is related to the quadratic penalty method, but it reduces the possibility of ill conditioning by introducing Lagrange multiplier estimates into the function to be minimized. The scalar μ is the penalty parameter and the vector λ is the vector of Lagrange multipliers. The Lagrangian function and its derivatives with respect to the displacements can be written as:

$$L(x,\lambda)=\sum_e\phi_e(x)+\sum_e\lambda_e\varphi_e(x)$$

$$\nabla_x L(x,\lambda)=\sum_e\nabla\phi_e(x)+\sum_e\lambda_e\nabla\varphi_e(x)$$

The augmented Lagrangian function and its derivatives with respect to the displacements can be written as:

$$L(x,\lambda,\mu)=\sum_e \phi_e(x)+\sum_e\left[\lambda_e+\frac{1}{2\mu}\varphi_e(x)\right]\varphi_e(x)$$

$$\nabla_x L(x,\lambda,\mu)=\sum_e \nabla\phi_e(x)+\sum_e\left[\lambda_e+\frac{1}{\mu}\varphi_e(x)\right]\nabla\varphi_e(x)$$

The following algorithm was adapted from [02] and [03]. The iterations terminate if the infinity norm of the gradient of the Lagrangian function becomes less than or equal to ε_l and the infinity norm of the constraint vector becomes less than or equal to ε_c.

6.2 Algorithm

$\mu \leftarrow \mu_0$

$\alpha \leftarrow \min(\mu,\gamma_1)$

$\omega \leftarrow \omega_0\alpha^{\alpha_\omega}$

$\eta \leftarrow \eta_0\alpha^{\alpha_\eta}$

$x \leftarrow x^0$

$\lambda \leftarrow \lambda^0$

While $\left\|\sum_e \nabla\phi_e(x)+\sum_e \lambda_e\nabla\varphi_e(x)\right\| > \varepsilon_l$ or $\|\varphi(x)\| > \varepsilon_c$ loop

Minimize $\sum_e \phi_e(x)+\sum_e\left[\lambda_e+\frac{1}{2\mu}\varphi_e(x)\right]\varphi_e(x)$

If $\|c(x)\| \le \eta$ then

$\lambda \leftarrow \lambda+\frac{1}{\mu}\varphi(x)$

$\alpha \leftarrow \min(\mu,\gamma_1)$

$\omega \leftarrow \omega\alpha^{\beta_\omega}$

$\eta \leftarrow \eta\alpha^{\beta_\eta}$

else

$\mu \leftarrow \tau\mu$

$$\alpha \leftarrow \min\left(\mu, \gamma_1\right)$$

$$\omega \leftarrow \omega_0 \alpha^{\alpha_\omega}$$

$$\eta \leftarrow \eta_0 \alpha^{\alpha_\eta}$$

end if

end loop

The typical parameter values are:

$$\alpha_\omega = 1,\ \beta_\omega = 1,\ \alpha_\eta < \min\left(1, \alpha_\omega\right) = 0.1,\ \beta_\eta < \min\left(1, \beta_\omega\right) = 0.9$$

$$\tau = 0.1,\ \omega_0 = 1,\ \eta_0 = 1,\ \gamma_1 = 0.1,\ \mu_0 = 0.1$$

7 Nonlinear Programming Problem

To find the local minimum points of a nonlinear multivariate function, the general strategy that can be used is: Choose a starting point and move in a given direction such that the function decreases. Find the minimum point in this direction and use it as a new starting point. Continue this way until a local minimum point is reached. The problem of finding the minimum points of a nonlinear multivariate function is replaced by a sequence of sub problems, each one consisting of finding the minimum of a univariate nonlinear function. In quasi-Newton methods, starting with the unit matrix, a positive definite approximation to the inverse of the Hessian matrix is updated at each iteration. This update is made using only values of the gradient vector. A direction such that the function decreases is calculated as minus the product of this approximation of the inverse of the Hessian matrix and the gradient vector calculated at the starting point of each iteration. Consequently, it is not necessary to solve any system of equations. Moreover, the analytical derivation of an expression for the Hessian matrix is not necessary. Note that by minimizing a function it is almost impossible to find a local maximum point. The only exception is that it is possible to find a saddle point, that is, the point is a local minimum and a local maximum. However, even in this improbable situation, a direction of negative curvature to continue toward a local minimum point can be found as described by [04]. The computer code uses the limited memory BFGS to tackle large scale problems as described by [05]. It also employs a line search procedure through cubic interpolation as described by [05].

8 Examples

The primary colors red, green, and blue are used for the line, triangle and tetrahedron elements, respectively. The secondary colors cyan, magenta, and yellow are used for the isovolumetric line, triangle and tetrahedron elements, respectively.

Example 1: An initially flat circular surface with thickness $\lambda = 2$, radius $r = 1$ and the boundary displaced according to the following hyperbolic paraboloid equation, where $h = 1/2$. Figure 4 shows the meshes for the initial and final surfaces. $\varepsilon_l = 10^{-4}$.

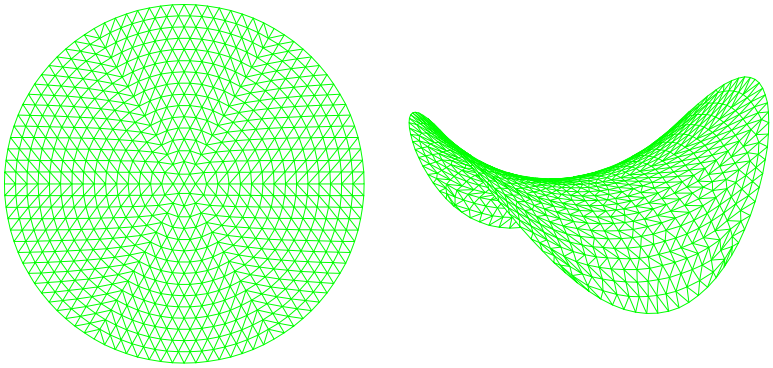

Figure 4

$$z = h\left[\left(\frac{x}{r}\right)^2 - \left(\frac{y}{r}\right)^2\right]$$

Example 2: A cylinder with thickness $\lambda = 1$, radius $r = 1$ and height $h = 1$. Figure 5 shows the meshes for the initial and final surfaces. $\varepsilon_l = 10^{-5}$.

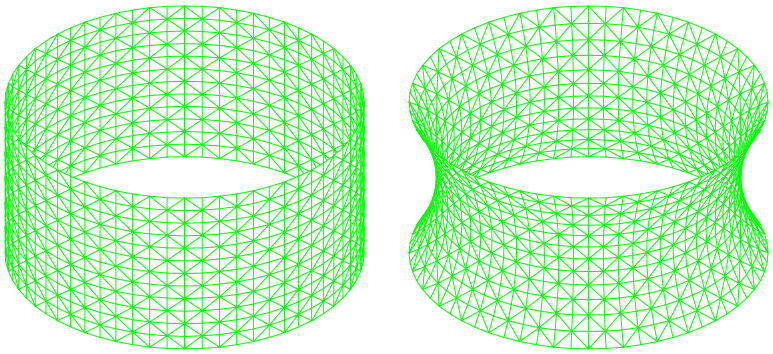

Figure 5

The final surface is symmetrical about the Z axis. The following analytical solution for the cross-section of the surface in the YZ plane is described by [06].

$$y(z) = c\cosh\left(\frac{z}{c}\right)$$

Note that $y(0) = c$. The value c is a solution of the following equation. In this example, $c = 0.8483379$.

$$\frac{2r}{h} = \frac{2c}{h}\cosh\left(\frac{h}{2c}\right)$$

Table 1 shows the relative error for c with different initial meshes.

Table 1

Elements	c	Error
384	0.8470554	0.15 %
1536	0.8480256	0.04 %
6144	0.8482543	0.01 %

Example 3: A frustum cone with thickness $\lambda = 2$, upper radius $r_2 = 0.5$, lower radius $r_1 = 1$ and height $h = 0.9$. Figure 6 shows the meshes for the initial and final surfaces. $\varepsilon_l = 10^{-5}$.

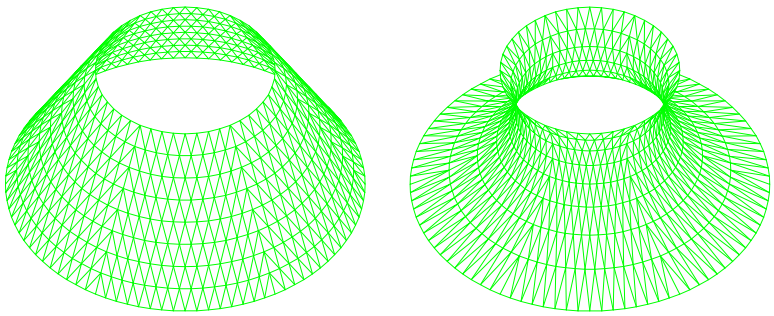

Figure 6

Example 4: On the top, Figure 7 shows an initial path through the corner points of a rectangle with horizontal dimension equal to 4 and vertical dimension equal to 2. The line elements have area $\alpha = 1$. On the bottom, Figure 7 shows the final path. $\varepsilon_l = 10^{-5}$.

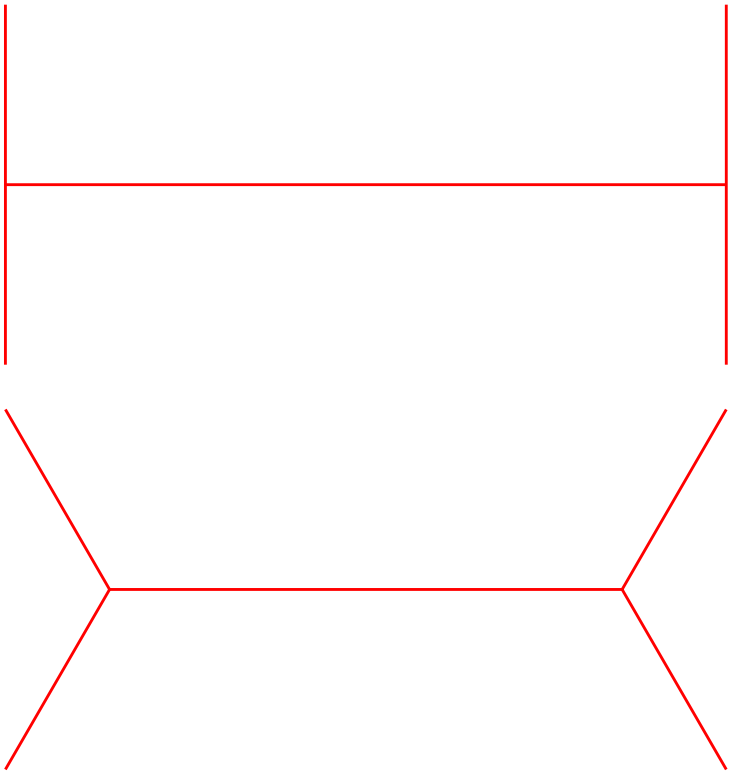

Figure 7

The general problem of connecting n points by the shortest path length is called Steiner problem [06]. Its solution contains straight lines intersecting at 120 degrees. The number of intersections is between 0 and $(n-2)$.

Example 5: An initially flat square surface with thickness $\lambda = 1$, side $s = 2$ and two opposite corners displaced by $+1/2$ while the two other opposite corners displaced by $-1/2$. The edges have line elements with area $\alpha = 5$. Figure 8 shows the meshes for the initial and final surfaces. $\varepsilon_l = 10^{-4}$.

Note that minimizing the total volume results in opposite effects on the lengths of the free edges. It tends to decrease the surface area defined by the triangle elements and consequently tends to increase the lengths of the free edges. It tends to decrease the path lengths defined by the line elements and consequently tends to decrease the lengths of the free edges. In this example, the free edges are curved due to relatively small value for the areas of the line elements.

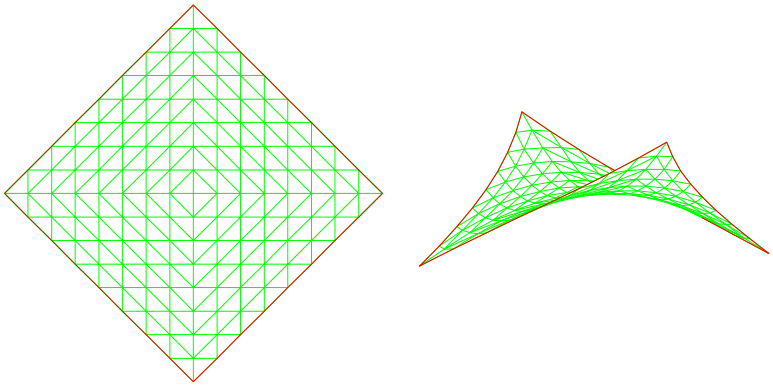

Figure 8

Example 6: An initially flat square surface with thickness $\lambda = 1$, side $s = 2$ and two opposite corners displaced by $+1/2$ while the two other opposite corners displaced by $-1/2$. The edges have line elements with area $\alpha = 500$. Figure 9 shows the meshes for the initial and final surfaces. $\varepsilon_l = 10^{-4}$.

Note that minimizing the total volume results in opposite effects on the lengths of the free edges. It tends to decrease the surface area defined by the triangle elements and consequently tends to increase the lengths of the free edges. It tends to decrease the path lengths defined by the line elements and consequently tends to decrease the lengths of the free edges. In this example, the free edges are straight due to relatively big value for the areas of the line elements.

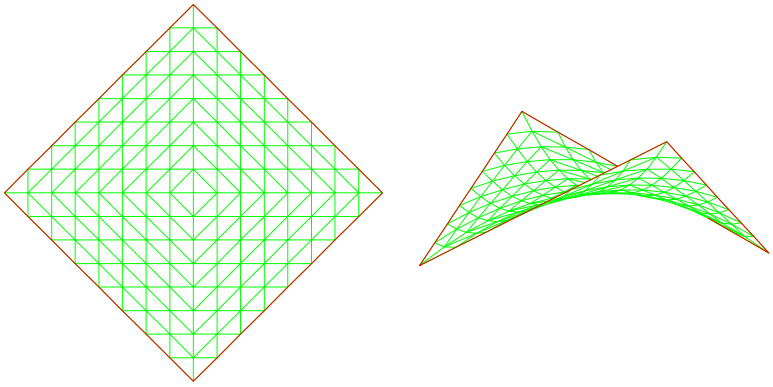

Figure 9

Example 7: A straight prismoid with height $h=3$. The bottom and top regular triangles are inscribed in a circle of radius $r=1$. It is composed by 3 line elements and 9 isovolumetric line elements. The line elements have area $\alpha=1$. The top triangle rotates 150 degrees clockwise relatively to the bottom triangle. Figure 10 shows the initial and final shapes. Appendix 1 presents analytical expressions for this type of prismoid. $\mu_0=10^{-3}, \varepsilon_l=10^{-5}, \varepsilon_c=10^{-6}$.

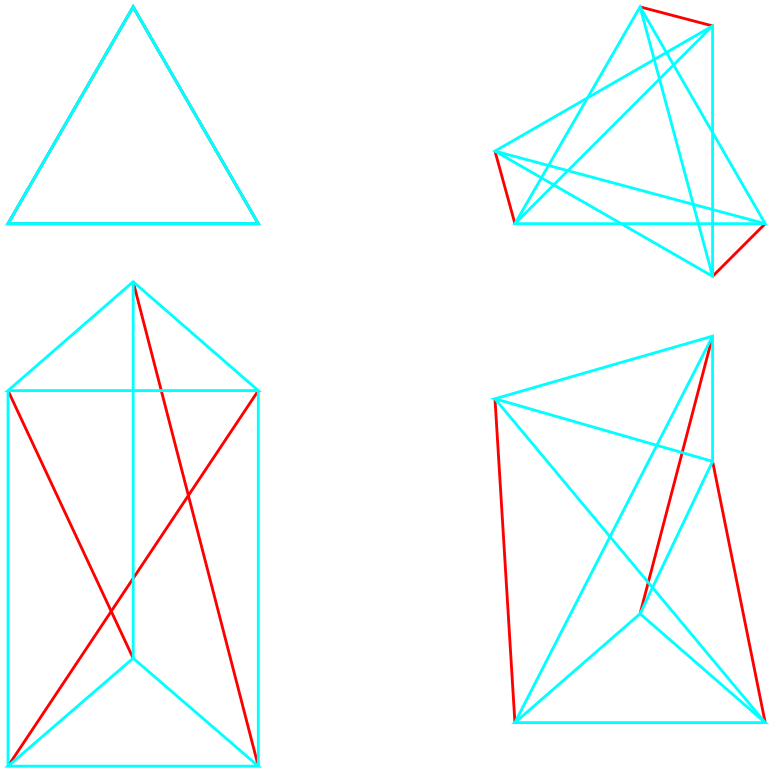

Figure 10

Example 8: A straight prismoid with height $h=2$. The bottom and top regular pentagons are inscribed in a circle of radius $r_1=0.75$ and $r_2=0.5$, respectively. It is composed by 5 line elements and 15 isovolumetric line elements. The line elements have area $\alpha=1$. The top pentagon rotates 126 degrees clockwise relatively to the bottom pentagon. Figure 11 shows the

initial and final shapes. Appendix 1 presents analytical expressions for this type of prismoid. $\mu_0 = 10^{-3}, \varepsilon_l = 10^{-5}, \varepsilon_c = 10^{-6}$.

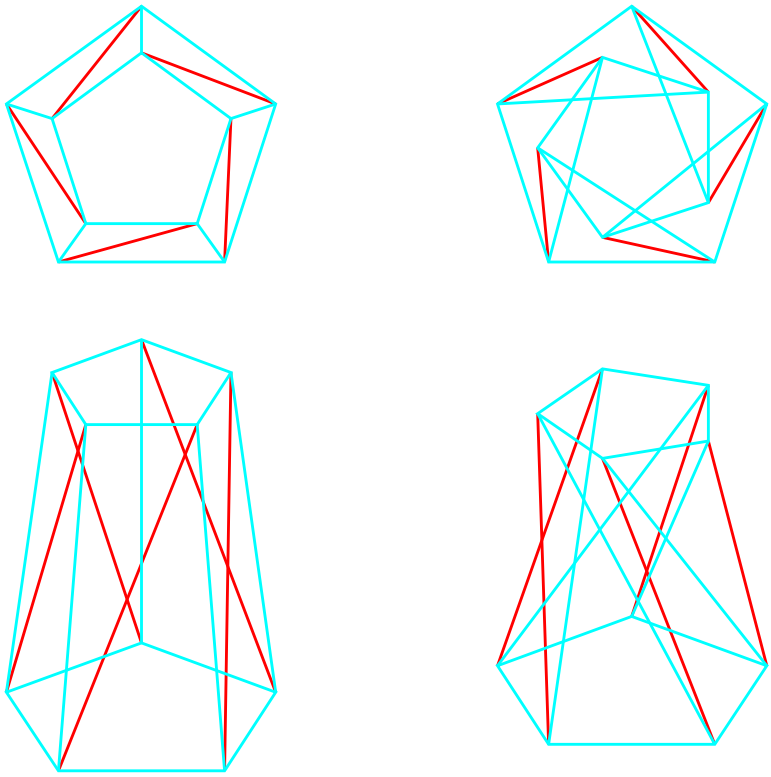

Figure 11

Example 9: A Stella Octangula as described in Appendix 2 with parameter $s = 1$ and support constraints on nodes 1, 2 and 3 to prevent rigid body motion. A nonregular Stella Octangula is generated by imposing different areas for selected elements of a regular Stella Octangula. Excluding the diagonal elements, all other elements are isovolumetric elements with area $\alpha = 1$. The areas for the diagonal elements in the initial shape and the lengths of the diagonal elements in the final shape are shown in Table 2.

Table 2

Elem	Area	Length
3	-1.25	1.4563
6	-1.50	1.5654
9	-1.75	1.6297
12	-2.00	1.8555
15	-2.25	1.8875
18	-2.50	1.8884

Figure 12 shows the initial shape (regular Stella Octangula) on the left and the final shape (nonregular Stella Octangula) on the right. $\mu_0 = 10^{-3}, \varepsilon_l = 10^{-3}, \varepsilon_c = 10^{-4}$.

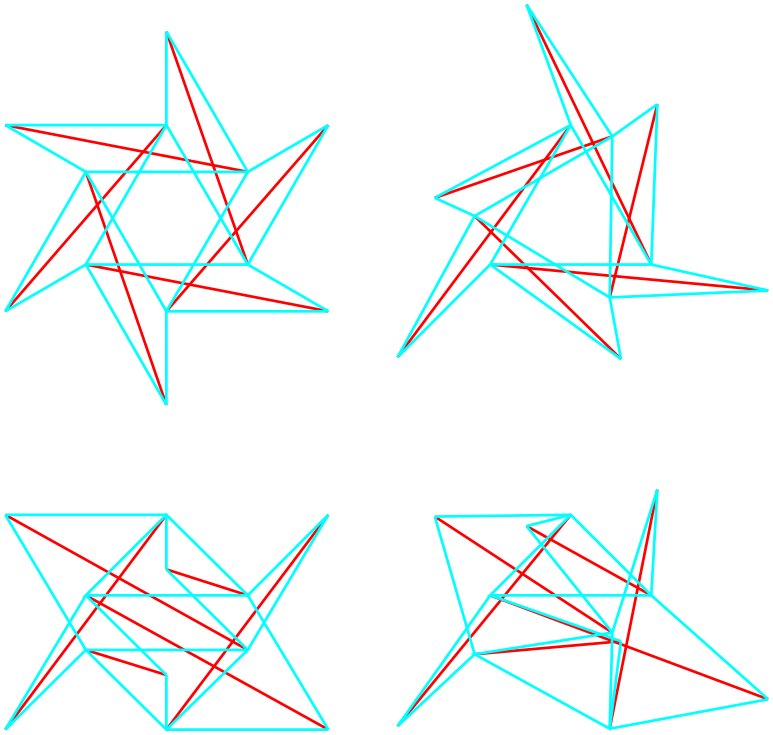

Figure 12

Example 10: The regular Stella Octangula is recovered by imposing equal areas for the same selected elements on the previously generated nonregular Stella Octangula. The areas for the diagonal elements in the initial shape and the lengths of the diagonal elements in the final shape are shown in Table 3.

Table 3

Elem	Area	Length
3	-1.00	1.7321
6	-1.00	1.7321
9	-1.00	1.7321
12	-1.00	1.7320
15	-1.00	1.7321
18	-1.00	1.7320

Figure 13 shows the initial shape (nonregular Stella Octangula) on the left and the final shape (regular Stella Octangula) on the right. $\mu_0 = 10^{-3}, \varepsilon_l = 10^{-3}, \varepsilon_c = 10^{-4}$.

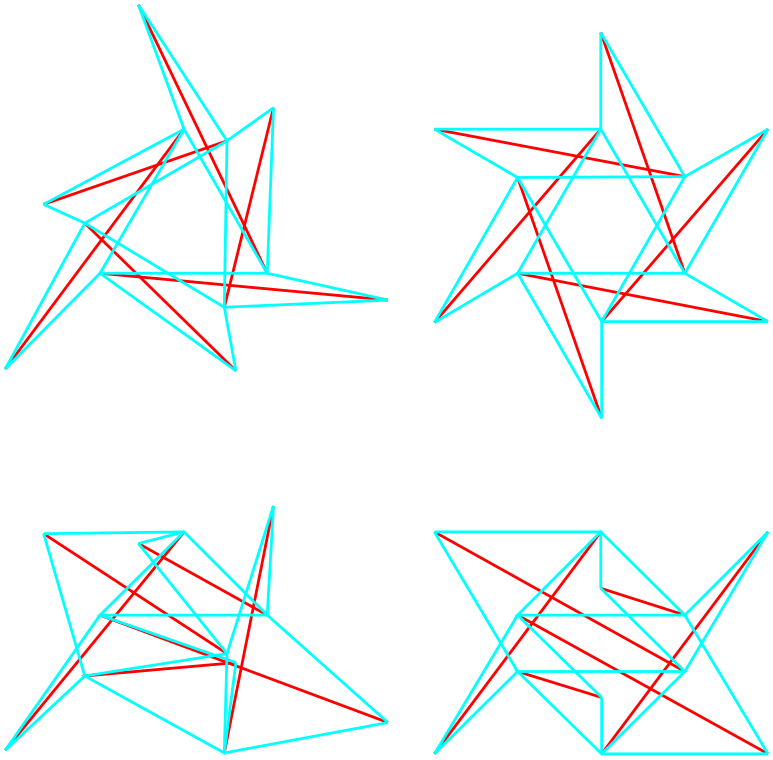

Figure 13

Example 11: A circular prismoid with axis on a circumference of radius $r=10$. The section is defined by a regular triangle inscribed in a circle of radius $r=1$. It is composed by 30 line elements and 60 isovolumetric line elements. The line elements have area $\alpha=1$. Figure 14 shows the initial and final shapes. $\mu_0=10^{-3}, \varepsilon_l=10^{-5}, \varepsilon_c=10^{-6}$.

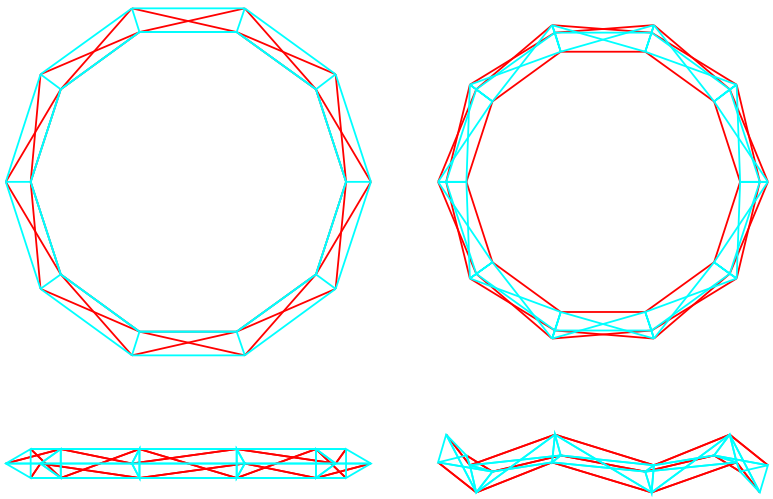

Figure 14

Example 12: A square with side $s=1$ composed by 8 isovolumetric triangle elements with thickness $\lambda=10$. The square's perimeter has line elements with area $\alpha=1$. The triangle

elements preserve the square's area while the line elements minimize its perimeter. The square turns into an octagon. Figure 15 shows the initial and final areas. $\mu_0 = 10^{-2}, \varepsilon_l = 10^{-5}, \varepsilon_c = 10^{-6}$.

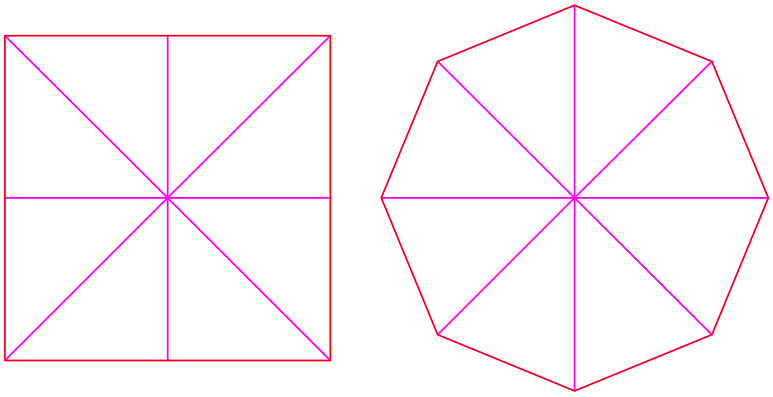

Figure 15

Example 13: A cube with side $s = 2$ composed by 24 isovolumetric tetrahedron elements. The cube's surface has triangle elements with thickness $\lambda = 1$. The tetrahedron elements preserve the cube's volume while the triangle elements minimize its surface. The cube turns into a 24 faces polyhedron. Figure 16 shows the initial and final volumes. $\mu_0 = 10^{-1}, \varepsilon_l = 10^{-6}, \varepsilon_c = 10^{-6}$.

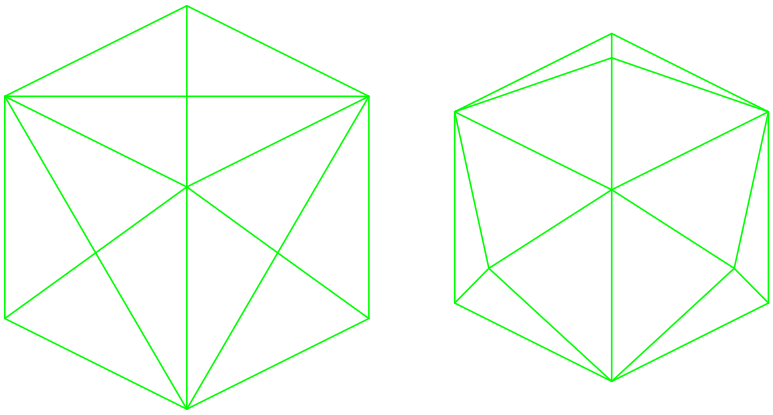

Figure 16

Example 14: Figure 17 shows the initial surface connecting two 12-sided polygon boundaries inscribed in non-coplanar ellipses. The boundary 1 is shown in cyan. The minor and major axes for ellipse 1 are equal to 1.0 and 0.8, respectively. The boundary 2 is shown in red. The minor and major axes for ellipse 2 are equal to 2.0 and 1.6, respectively. The minor axes are parallel. The major axes are contained in a plane orthogonal to ellipse 2. The left vertex of ellipse 1 is the surface apex and it is located at (-0.15, 0, 0.6) from the center of ellipse 2. The right vertex of ellipse 1 is located on a line from the apex to the right vertex of ellipse 2. The boundary 1 is composed by 36 isovolumetric line elements with area $\alpha = 1.0$. The boundary 2 is composed by 144 line elements with area $\alpha = 0.1$. The surface thickness is $\lambda = 0.1$. The apex and the ellipse 2 vertices are fixed points. Figure 18 shows the final surface. $\mu_0 = 10^{-3}, \varepsilon_l = 10^{-3}, \varepsilon_c = 10^{-6}$.

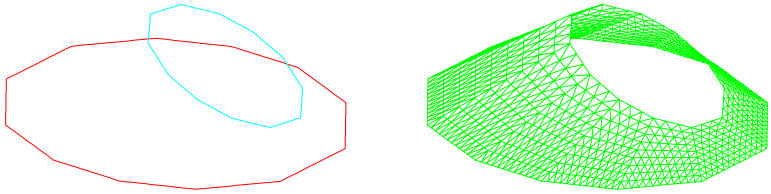

Figure 17

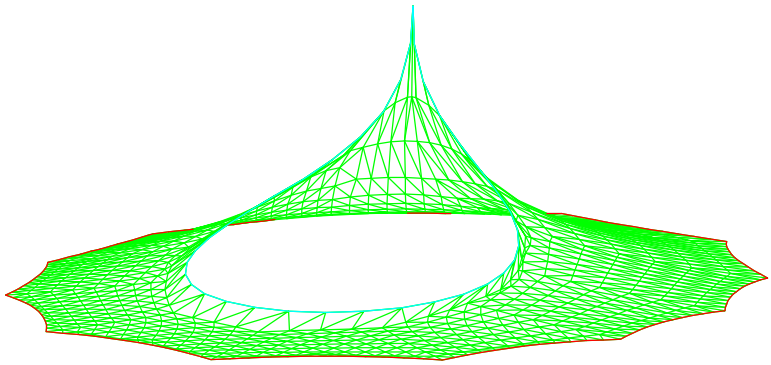

Figure 18

9 Appendix 1

Figure 19 shows a straight prismoid. The bottom and top regular polygons are inscribed in circles of different radius. The sum of the lengths of the red lines is minimized by rotating the top polygon counterclockwise with respect to the bottom polygon, while the lengths of the black lines remain constant.

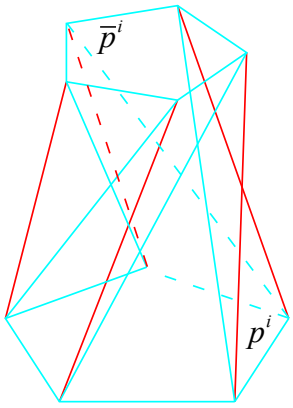

Figure 19

9.1 Geometry

For n-sided regular polygons, the coordinates of the vertices can be written as:

$$\gamma = \frac{2\pi}{n}$$

$$p^i = \begin{bmatrix} r\cos(\gamma i) \\ r\sin(\gamma i) \\ 0 \end{bmatrix}$$

$$\overline{p}^i = \begin{bmatrix} \overline{r}\cos(\theta + \gamma i) \\ \overline{r}\sin(\theta + \gamma i) \\ h_\theta \end{bmatrix}$$

$$b^i = p^{i+1} - p^i$$

$$d^i = \overline{p}^i - p^{i+1}$$

$$v^i = \overline{p}^i - p^i$$

9.2 Final height

The square of the norm of vector v^i can be written as:

$$v^i = \overline{p}^i - p^i \Rightarrow$$

$$\left\| v^i \right\|^2 = \overline{r}^2 + r^2 - 2\overline{r}r\cos\theta + h_\theta^2$$

Since this norm is constant, it leads to the following expression that relates the initial and final heights.

$$h_\theta^2 = h_0^2 - 2\overline{r}r\left(1 - \cos\theta\right)$$

9.3 Rotation angle

The square of the norm of vector d^i can be written as:

$$b^i + d^i - v^i = 0 \Rightarrow$$

$$\left\| d^i \right\|^2 = \left\| v^i \right\|^2 + \left\| b^i \right\|^2 - 2r^2\left(1 - \cos\gamma\right) - 2r\overline{r}\left[\cos\left(\theta - \gamma\right) - \cos\theta\right]$$

Due to symmetry, minimizing the sum of the norms of all vectors is equivalent to minimizing the square of the norm of only one vector.

$$\frac{\partial \left\| d^i \right\|^2}{\partial\theta} = 0 \Rightarrow \tan\theta = \frac{\sin\gamma}{\cos\gamma - 1}$$

Note that this expression is valid when the vectors connect the corresponding bottom and top points in any symmetric way. Table 4 shows the rotation angle in degrees and the values for the relation between the initial and final heights for some n-sided regular polygons.

$$\rho = \frac{h_0^2 - h_\theta^2}{\overline{r}r} = \left(2 - 2\cos\gamma\right)^{\frac{1}{2}} + 2$$

Table 4

n	θ	ρ
3	150.0	3.732051
4	135.0	3.414214
5	126.0	3.175571
6	120.0	3.000000
7	115.7	2.867767
8	112.5	2.765367
9	110.0	2.684040
∞	90.0	2.000000

9.4 Minimum initial height

The minimum initial height is given by:

$$h_0^2 \geq \overline{r}r\left(2 - 2\cos\gamma\right)^{\frac{1}{2}} + 2\overline{r}r \Rightarrow h_\theta \geq 0$$

10 Appendix 2

Figure 20 shows the geometry of a sculpture called Stella Octangula, which was proposed by David Georges Emmerich. He was a Hungarian architect, sculptor, and author. An extensive description of his works is given by [07].

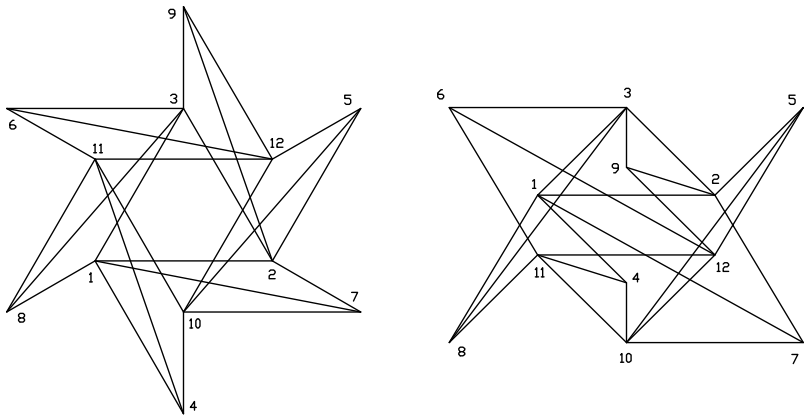

Figure 20

The geometry is composed by 18 elements with length equal to s and 6 diagonal elements with length equal to $s\sqrt{3}$. Table 5 shows the coordinates of the vertices, where the parameters r and h are given by:

$$r = \frac{s}{\sqrt{3}}$$

$$h = \frac{s}{\sqrt{6}}$$

Table 5

Node	Coord-X	Coord-Y	Coord-Z
1	$-s/2$	$-r/2$	$+h$
2	$+s/2$	$-r/2$	$+h$
3	0	$+r$	$+h$
4	0	$-2r$	$+h$
5	$+s$	$+r$	$+h$
6	$-s$	$+r$	$+h$
7	$+s$	$-r$	$-h$
8	$-s$	$-r$	$-h$
9	0	$+2r$	$-h$
10	0	$-r$	$-h$
11	$-s/2$	$+r/2$	$-h$
12	$+s/2$	$+r/2$	$-h$

Table 6 shows the connectivity of the diagonal elements.

Table 6

Elem	Node	Node
3	4	11
6	5	10
9	6	12
12	7	1
15	8	3
18	9	2

11 Appendix 3

$$a^T\left(b\times c\right) = b^T\left(c\times a\right) = c^T\left(a\times b\right)$$

$$v = a\times x \Rightarrow \begin{bmatrix} \frac{\partial v_1}{\partial x_1} & \frac{\partial v_1}{\partial x_2} & \frac{\partial v_1}{\partial x_3} \\ \frac{\partial v_2}{\partial x_1} & \frac{\partial v_2}{\partial x_2} & \frac{\partial v_2}{\partial x_3} \\ \frac{\partial v_3}{\partial x_1} & \frac{\partial v_3}{\partial x_2} & \frac{\partial v_3}{\partial x_3} \end{bmatrix} = \begin{bmatrix} 0 & -a_3 & a_2 \\ a_3 & 0 & -a_1 \\ -a_2 & a_1 & 0 \end{bmatrix}$$

References

[01] Goldberg D (1991) What Every Computer Scientist Should Know About Floating-Point Arithmetic. ACM Comput Surv doi:10.1145/103162.103163

[02] Conn AR, Gould NIM, Toint PL (1991) A globally convergent augmented lagrangian algorithm for optimization with general constraints and simple bounds. Siam J Numer Anal doi.org/10.1137/0728030.

[03] Conn AR, Gould NIM, Toint PL (2010) Lancelot: A Fortran Package for Large-Scale Nonlinear Optimization. Springer

[04] Gill PE, Murray W (1974) Newton type methods for unconstrained and linearly constrained optimization. Math Program doi:10.1007/BF01585529

[05] Nocedal J, Wright SJ (2006) Numerical optimization. Springer-Verlag

[06] Isenberg C (1992) The Science of Soap Films and Soap Bubbles. Dover Publications

[07] Chassagnoux A (2006) David Georges Emmerich Professor of morphology. Int J Space Struct doi: 10.1260/026635106777641144